

EXTRACTION OF COAL TAR ABSORPTION OIL BY A CONTINUOUS COUNTER CURRENT SPRAY COLUMN

Student Number: 04M18127 Name: Saito Jun Supervisor: Egashira Ryuichi

連続式向流接触スプレー塔によるコールタール吸収油の抽出分離 齋藤 潤

コールタール蒸留留分の一つである吸収油中の含窒素成分（キノリン，イソキノリン，インドール）とその他の成分（同素環式化合物など）の抽出分離に対しスプレー塔型接触装置を適用した。溶媒の組成，両相の流量，などの条件を変化させて，原料吸収油（重液，分散相）と溶媒であるメタノール水溶液（軽液，連続相）を向流に接触させ定常状態に至らせた。良好な向流接触操作が可能であり，含窒素成分の収率および他の成分に対する分離の選択性は，それぞれ最大で 0.3 および 30 程度であった。また，物質移動抵抗は連続相側が支配的であった。

1. Introduction

Coal tar, one of the byproducts from coal carbonization, contains many useful compounds to chemical industry. First, coal tar is separated into several fractions by distillation. Absorption oil (abbreviated to AO) which is one of these fractions (b.p.=470~550K) contains nitrogen heterocyclic compounds (nitrogen compounds) such as quinoline (Q), isoquinoline (IQ), indole (IL), etc, and the other compounds such as naphthalene (N), 1-methylnaphthalene (1MN), 2-methylnaphthalene (2MN), biphenyl (BP), dibenzofuran (DBF) etc. Generally, the current method mainly used to separate these compounds in AO is reactive extraction by acid and/or base. However, this process is relatively costly because the acid and base used as solvent are very difficult to be recovered and cause corrosion of the equipments. For the separation problems, the solvent extraction with aqueous methanol (MeOH aq.) etc¹⁻⁸⁾ has been suggested. The process proposed is based on the liquid-liquid equilibriums of the components and there are no studies concerning about practical contactors and mass transfer rates. Spray columns are the simplest differential-contact devices in laboratory studies. Their advantages are that the throughput is large and the interfacial area is directly measurable. In this study, a countercurrent spray column was applied to separation of AO as a continuous apparatus in practical use and operability, separation performances including mass transfer rates, and so forth were examined.

2. Experimental

Schematic diagram of the apparatus used in continuous operation is shown in Fig. 1. The column is made of pyrex glass and behavior in the column can be observed. Figure 2 shows details of distributors. The distributor of dispersed phase has 8 needle nozzles. The distributor of continuous phase has outlets on side of cylinder to pretend falling disperse drops entering in it. The experimental procedure is below. First, feed

(AO) and solvent (MeOH aq.) were stocked in the tanks. The column top and bottom were continuously fed with AO as the dispersed phase and MeOH aq. as the continuous phase respectively and the two fluids were contacted countercurrently. The inlet flow rates were kept constant by checking the flow indicators and the level of the interface between the continuous phase and accumulated raffinate phase at the bottom was maintained by adjusting the drain valve of raffinate phase. The inlet and outlet flow rates were determined by weighing outlet mass per unit time, respectively. The holdup of dispersed phase in the column was obtained by measuring the ascent of interface between continuous phase and accumulated raffinate phase at the bottom when the AO inlet and drain were closed at the same time. AO, solvent, raffinate, and extract phase were

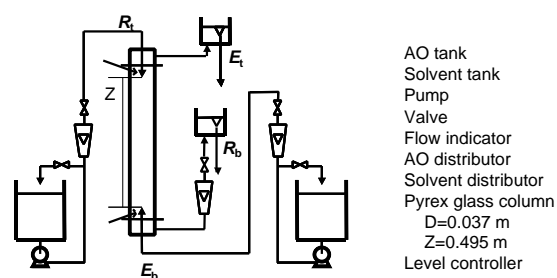


Fig.1 Schematic diagram of the experimental apparatus

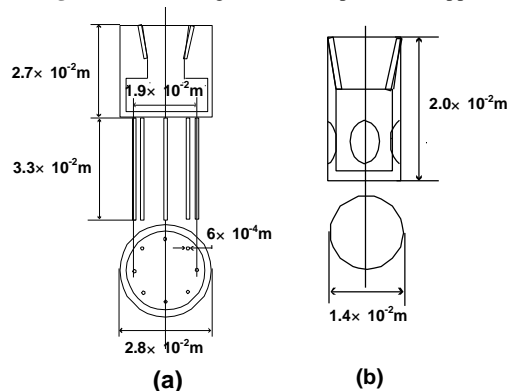


Fig. 2 Details of distributors;

(a) for dispersed phase; (b) for continuous phase

analyzed by GC⁶⁾ and Karl Fischer's titration was conducted to give the water content. The densities of these phases were measured with the pycnometers. The principal experimental conditions are summarized in **Table 1**. Water content in the solvent, $y_{w,b}$, and inlet flow rates, E_b , and R_t , were changed.

Table.1 Experimental conditions

No	feed:absorption oil R_t [kg·hr ⁻¹ ·m ⁻²]	solvent:aqueous methanol $y_{w,b}$ [-]	E_b [kg·hr ⁻¹ ·m ⁻²]
EC1	$4 \times 10^2 \sim 3 \times 10^3$	0.3	1×10^3
EC2	$5 \times 10^2 \sim 5 \times 10^3$	0.5	1×10^3
EC3	$4 \times 10^2 \sim 4 \times 10^3$	0.3	2×10^3
EC4	$4 \times 10^2 \sim 5 \times 10^3$	0.5	2×10^3

The liquid-liquid equilibrium relationships were measured for estimating the mass transfer rates.

3. Result and discussion

3.1. Basic results

3.1.1. Liquid-liquid equilibrium

The liquid-liquid equilibrium relationships obtained in this study were equal to those in the previous study⁶⁾.

3.1.2. Density

The densities of materials are summarized in **Table 2**. The density of dispersed phase was larger than that of extract phase. The density changes did not effect seriously on continuous operation. The density of continuous phase in the runs with $y_{w,b} = 0.5$ was larger than that in those with 0.3.

Table.2 Densities of the materials

Materials	Density [kg·m ⁻³]
absorption oil	1.1×10^3
methanol	7.9×10^2
aqueous methanol ($y_{w,b} = 0.3$)	8.7×10^2
aqueous methanol ($y_{w,b} = 0.5$)	9.2×10^2
raffinate phase	1.1×10^3
extract phase ($y_{w,b} = 0.3$)	$8.8 \sim 8.9 \times 10^2$
extract phase ($y_{w,b} = 0.5$)	$9.2 \sim 9.3 \times 10^2$

3.2. Numerical relationships

The holdup of dispersed phase in the column, H , was defined by

$$H = V_d / V \quad (1)$$

The V_d and V in the equation were the volume of disperse phase in the column and the column volume, respectively. One can write the material balance relationship in terms of the mass change rates of constituents i in respective phases with the mass fractions, as follows:

$$R_t \cdot x_{i,t} - R_b \cdot x_{i,b} = E_t \cdot y_{i,t} - E_b \cdot y_{i,b} \quad (2)$$

The yield, Y_i , and separation selectivity relative to 2MN of component i , $\beta_{i/2MN}$, were defined by,

$$Y_i = E_t \cdot y_{i,t} / R_t \cdot x_{i,t} \quad (3)$$

$$\beta_{i/2MN} = (y_{i,t} / y_{2MN,t}) / (x_{i,b} / x_{2MN,b}) \quad (4)$$

The overall coefficient of mass transfer based on the

concentration in continuous phase, $K_{c,i}$, was calculated by,

$$d(R \cdot x_i) / dz = -K_{c,i} \cdot a \cdot (y_i^* - y_i) \quad (5)$$

with the boundary conditions of top and bottom of the column. y_i^* in this equation was estimated from x_i with using the equilibrium relationships. a and z were specific interfacial area between continuous phase and disperse phase and distance from top of the column, respectively.

3.3. Behavior in the column

In all the runs, entrainment of the dispersed phase particles into the continuous phase and flooding were not observed and then countercurrent contact could be carried out favorably. The diameters of dispersed phase drops were larger in the runs with $y_{w,b} = 0.5$ than in those with 0.3 because the differences of densities between continuous and dispersed phase were smaller (see Table 2). The drop diameters decreased, as the flow rate of dispersed phase, R_t , increased (see **Fig. 3**). The coalescence of the dispersed phase and axial mixing were observed in the range of higher R_t . Holdup of dispersed phase in the column, H , shows in **Fig. 4**. E_b and $y_{w,b}$ had no effect on H . Therefore the flow rates of both phases were under the loading point. **Figure 5** shows the specific interfacial area, a , plotted against R_t .

3.4. Composition

The compositions of feed AO are shown in **Table 3**. **Figure 6** shows the extract compositions, $y_{i,t}$, plotted against R_t . The substantial mass transfers of studied compounds could be detected with this bench scale column of which effective contact height was 0.495 m. In all the runs, $y_{i,t}$ increased with increasing R_t . The nitrogen compounds transferred from feed into extract phase preferentially to the other compounds and the separation between these compounds could be achieved. In the low range of R_t , $y_{i,t}$ were smaller in the runs with $E_b=2000$ than in those with 1000, but the differences became small with increasing R_t . It was because two phases in the column almost reached equilibrium in the high range R_t ,

Table 3 Compositions of feed oil

Composition in mass fraction			
quinoline	$x_{Q,t}$	[-]	0.05 ~ 0.09
isoquinoline	$x_{IQ,t}$	[-]	0.02 ~ 0.03
indole	$x_{IL,t}$	[-]	0.04 ~ 0.06
naphthalene	$x_{N,t}$	[-]	0.02 ~ 0.03
1-methylnaphthalene	$x_{1MN,t}$	[-]	0.09 ~ 0.1
2-methylnaphthalene	$x_{2MN,t}$	[-]	0.2 ~ 0.3
biphenyl	$x_{BP,t}$	[-]	0.06 ~ 0.09
dibenzofuran	$x_{DBF,t}$	[-]	0.06 ~ 0.1
water	$x_{w,t}$	[-]	0 ~ 0.004
methanol	$x_{MeOH,t}$	[-]	0 ~ 0.04

3.5. Yield and selectivity

Figure 7 shows the yields Y_i against R_t . Y_i were bigger in the runs with $y_{i,w} = 0.3$ than in those with 0.5 for the equilibrium relationship. In the range of this work, Y_i of the nitrogen compounds were about 0.4 at maximum with this column,

while those of the other components were below 0.1. **Figure 8** shows the separation selectivity, $b_{i/2MN}$ against R_t . $b_{i/2MN}$ of the nitrogen compounds were larger in the run with $y_{w,b} = 0.5$ than in those with 0.3 and about 30 at maximum.

3.6. Overall mass transfer coefficient

Figure 9 shows the overall volumetric mass transfer coefficients based on the concentration in continuous phase, $K_{c,i}a$, against R_t . $K_{c,i}a$ increased with R_t , mainly due to the decrease of diameter of dispersed phase drops and then that of the increase of specific interfacial area, a . The effects of R_t on the overall mass transfer coefficient based on the concentration in the continuous phase, $K_{c,i}$, are shown in **Fig. 10**. The axial mixing was observed in the high range of R_t . $K_{c,i}$ decreased with increasing R_t because concentration differences became smaller compared with the case to assume the plug flow in the column. $K_{c,i}$ in the case of higher solvent flow rate, E_t , was larger than those at the lower E_t . Therefore, the laminar film in continuous phase controlled the mass transfers.

4. Conclusion

The extraction separation of absorption oil with the continuous apparatus was carried out favorably under the conditions in this study. The yields, Y_i , and selectivity, $\beta_{i/2MN}$, of them were about 0.4 and 30 at maximum, respectively. The mass transfers were explained in term of mass transfer coefficients. The overall mass transfer coefficient based on the concentration in the continuous phase, $K_{c,i}$, decreased with increasing R_t because axial mixing occurred in the column. The mass transfer resistance existed mainly in continuous phase. Consequently, the useful information for the process design was provided.

Acknowledgment

AO was provided by JFE Chemical Corporation.

Nomenclatures

a : specific interfacial area [m²·m⁻³]
 E : superficial mass flow rate of aqueous phase [kg·hr⁻¹·m⁻²]
 H : holdup of the dispersed phase [-]
 K_c : overall mass transfer coefficient based on the concentration in continuous phase [kg·hr⁻¹·m⁻²]
 R : superficial mass flow rate of oil phase [kg·hr⁻¹·m⁻²]
 V : volume in the column [m³]
 x : mass fraction in oil phase [-]
 y : mass fraction in aqueous phase [-]
 Y : yield [-]
 z : distance from top of the column [m]
 Z : effective contact height of column [m]
 $b_{i/2MN}$: separation selectivity of component i relative to 2-methylnaphthalene [-]

<Subscripts>

1MN : 1-methylnaphthalene

2MN : 2-methylnaphthalene

b : at bottom of the column

BP : biphenyl

DBF : dibenzofuran

IL : indole

IQ : isoquinoline

i : component i

MeOH: methanol

N : naphthalene

Q : quinoline

t : at top of the column

W : water

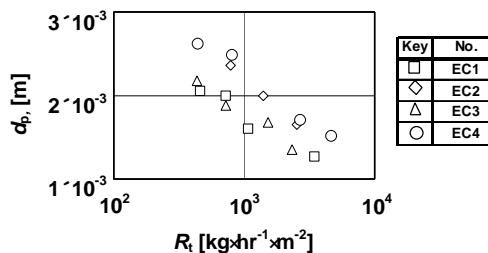


Fig. 3 Diameters of the dispersed phases

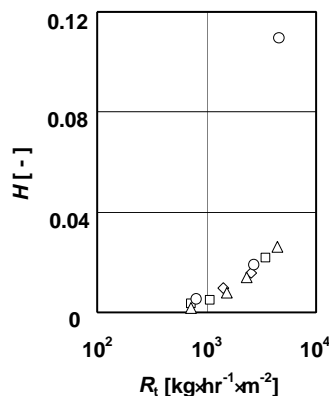


Fig. 4 Holdup of the dispersed phase, H : (the keys are the same as Fig. 3)

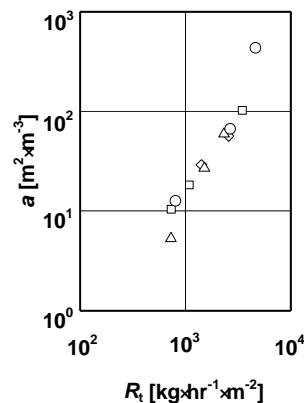


Fig. 5 specific interfacial area, a : (the keys are the same as Fig. 3)

Key	Run	i									
◇	EC1	Q	▷	EC1	1MN	▣	EC1	IL	▣	EC1	BP
◆	EC2		▷	EC2		▣	EC2		▣	EC2	
◇	EC3		▷	EC3		▣	EC3		▣	EC3	
◇	EC4		▷	EC4		▣	EC4		▣	EC4	
△	EC1	IQ	▷	EC1	2MN	◇	EC1	N	◇	EC1	DBF
▲	EC2		▷	EC2		◇	EC2		◇	EC2	
△	EC3		▷	EC3		◇	EC3		◇	EC3	
▲	EC4		▷	EC4		◇	EC4		◇	EC4	

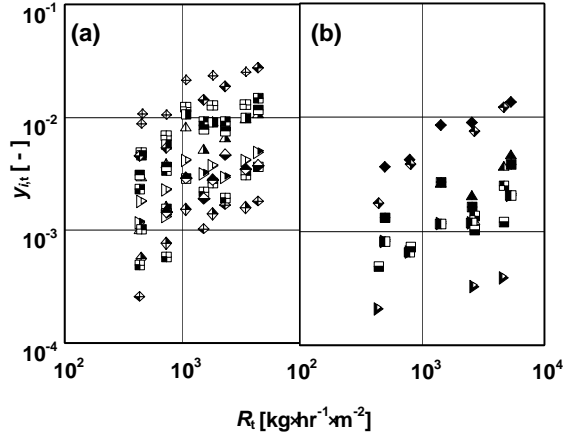


Fig. 6 Extract compositions, y_{it} :(a) in EC1 and 3; (b) in EC2 and 4

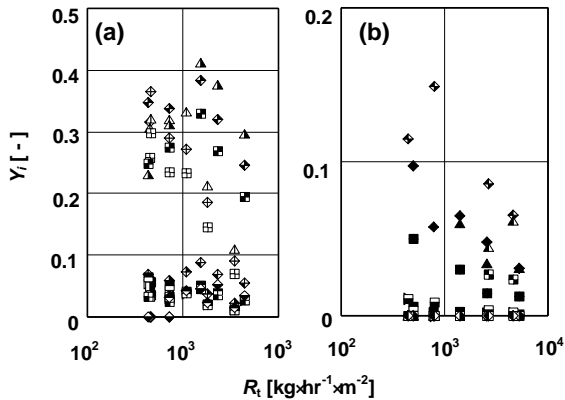


Fig. 7 Yields, Y_i :(a) in EC1 and 3; (b) in EC2 and 4 (the keys are the same as Fig. 6)

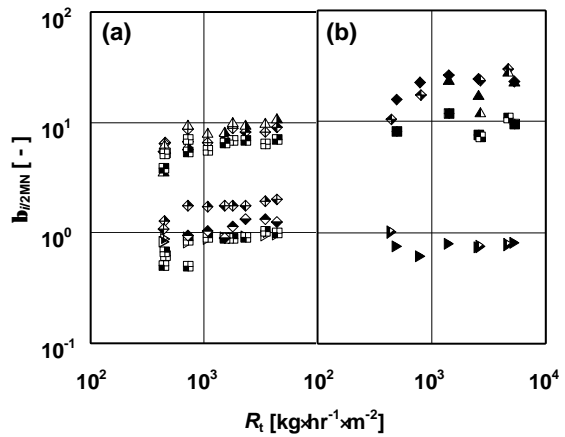


Fig. 8 Separation selectivity, $b_{i/2MN}$:(a) in EC1 and 3; (b) in EC2 and 4 (the keys are the same as Fig. 6)

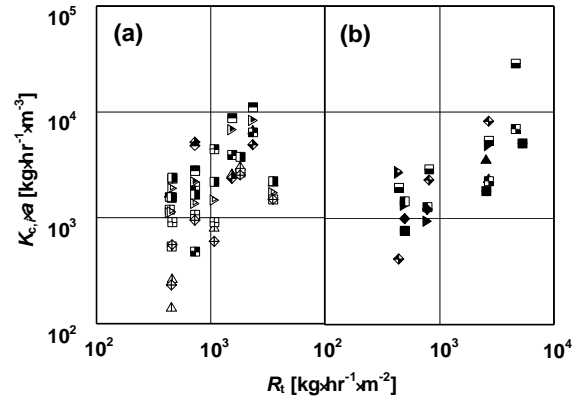


Fig. 9 Overall volumetric mass transfer coefficients based on the concentration in continuous phase, $K_{c,i} \alpha$:(a) in EC1 and 3; (b) in EC2 and 4(the keys are the same as Fig. 6)

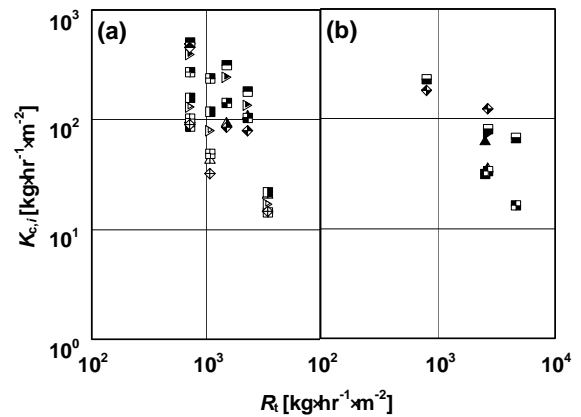


Fig. 10 Overall mass transfer coefficients based on the concentration in continuous phase, $K_{c,i}$:(a) in EC1 and 3; (b) in EC2 and 4 (the keys are the same as Fig. 6)

Reference

- 1) Ukegawa, K., Matsumura, A., Kodera, Y., Kondo, T., Nakayama, T., Tanabe, H., Yoshida, S., Mito, Y., *Sekiyu Gakkaishi (J. Jpn. Petrol. Inst.)*, **33**, (4), 250 (1990).
- 2) Kodera, Y., Ukegawa, K., Mito, Y., Komoto, M., Ishikawa, E., Nagayama, T., *Fuel*, **70**, (6), 765 (1991).
- 3) Matsumura, A., Kodera, Y., Kondo, T., Ukegawa, K., Tanabe, H., Yoshida, S., Mito, Y., *Shigen to Kankyo (Journal of NIRE)*, **4**, (2), 147 (1995)
- 4) Egashira, R., Nagai, M., *Sekiyu Gakkaishi (J. Jpn. Petrol. Inst.)*, **43**, (5), 339 (2000)
- 5) Egashira, R., Salim, C., *Sekiyu Gakkaishi (J. Jpn. Petrol. Inst.)*, **44**, (3), 178 (2001)
- 6) Salim, C., Saito, J., Egashira, R., *Journal of the Japan Petroleum Institute*, **48**, (1), 60 (2005)
- 7) Watanabe, K., Egashira, R., 34th Japan Petroleum Institute meeting, (2004)
- 8) Salim, C. Dissertation for a doctoral degree of engineering, Tokyo Institute of Technology (2005)